205

EVALUATION OF PHOTON CONTAMINATION IN DEGRADED ELECTRON BEAMS

A Thesis

Submitted to the Graduate Faculty of the
Louisiana State University and
Agricultural and Mechanical College
in partial fulfillment of the
requirements for the degree of

Master of Science

in

Nuclear Science

(Medical Radiation Science Option)

by

Alan G. Douglas
B.S., B.A., North Carolina Wesleyan College, 1971

December, 1983

DEDICATED TO

my wife, Nancy

ACKNOWLEDGEMENT

The author would like to express his sincere appreciation to his major co-professors, W. J. Kubricht, Jr., M.S. and Sheldon A. Johnson, M.D. for their assistance, encouragement, advice and guidance throughout the preparation of this work.

The author is thankful to the staff of the Nuclear Science Center, Dr. Edward N. Lambremont, Dr. Robert C. McIlhenny and Dr. Ronald M. Knaus for their advice and encouragement.

Special appreciation is expressed to Robert Shalek, Ph.D. of the University of Texas M.D. Anderson Hospital and Tumor Institute for taking the time from his busy schedule to listen, advise, critique and serve as a member of the examining committee.

A note of thanks is given to Mrs. Evalyn Horton and Mrs. Diane Zeigler for their time deciphening, correcting and typing this manuscript.

The author wishes to express to his wife his appreciation for her steadfast faith and love. These are the foundation upon which all else is built.

TABLE OF CONTENTS

LIST OF FIGURES

ABSTRACT

Total-skin electron beam therapy for certain malignant diseases such as mycosis fungoides is becoming more commonplace with the increasing availability of linear accelerators with electron beam capability. The electron beam energies supplied on commercial accelerators are often too high for direct total-skin irradiation. These beams are degraded to lower energies by interposing low atomic-number materials in the electron beam. The inevitable bremsstrahlung (photon) contamination is investigated to determine the source of the contamination and the hazard to the patients. The fraction of bremsstrahlung in the electron beam is determined in several different geometries using ion chamber measurements. Angling the electron beam above and below the treatment volume reduced, to the greatest extent, the contamination observed by directing the photons away from the radiation detector. The placement of the beam degrading material near the detector was found to yield much lower contamination and greater electron flux than positioning it near the accelerator collimator.

INTRODUCTION

In radiation oncology, which is the use of radiation for the treatment of cancer, the two radiations of primary importance are photons and high energy electrons. The use of high energy electrons has increased greatly in the last several years because of the availability of linear accelerators that have electron beam capability.[1] Electrons have a comparatively large coulombic charge relative to their small mass. This characteristic accounts for their large-angle scattering and limited range in matter. For instance, Figure 1 compares 4 million volt (4 MV) x-rays and 6 million electron volt (6 MeV) electrons, where the percent of maximum ionization is shown relative to the depth in water. At 3 cm, the electrons have given up virtually all of their energy but the photon beam is still at more than 90% of its maximum value. This characteristic lack of penetrability by electrons has a distinct advantage in the treatment of certain diseases. One such disease is mycosis fungoides, a cutaneous malignancy that involves primarily the upper dermis and the epidermis.

The treatment regimen for the disease involves total skin irradiation with an electron beam, which because of their poor penetrability spare deeper tissues from radiation damage. The rapid decrease in electron fluence with depth spares internal critical organs, but at the same time, the malignant tissues are being effectively irradiated.

To treat mycosis fungoides adequately with radiation, it is necessary to treat the body surface only to those depths which contain the malignant cells. These malignant cells generally lie within 1 cm of the surface. Therefore, an electron energy must be selected to limit the depth of penetration to approximately 1 cm. The normally prescribed dose for mycosis fungoides is in the range of 2000 to 4000 rads given at a rate of 500 rads per week. The average dose is around 3500 rads. If the dose at 1 cm depth is within 85% of the

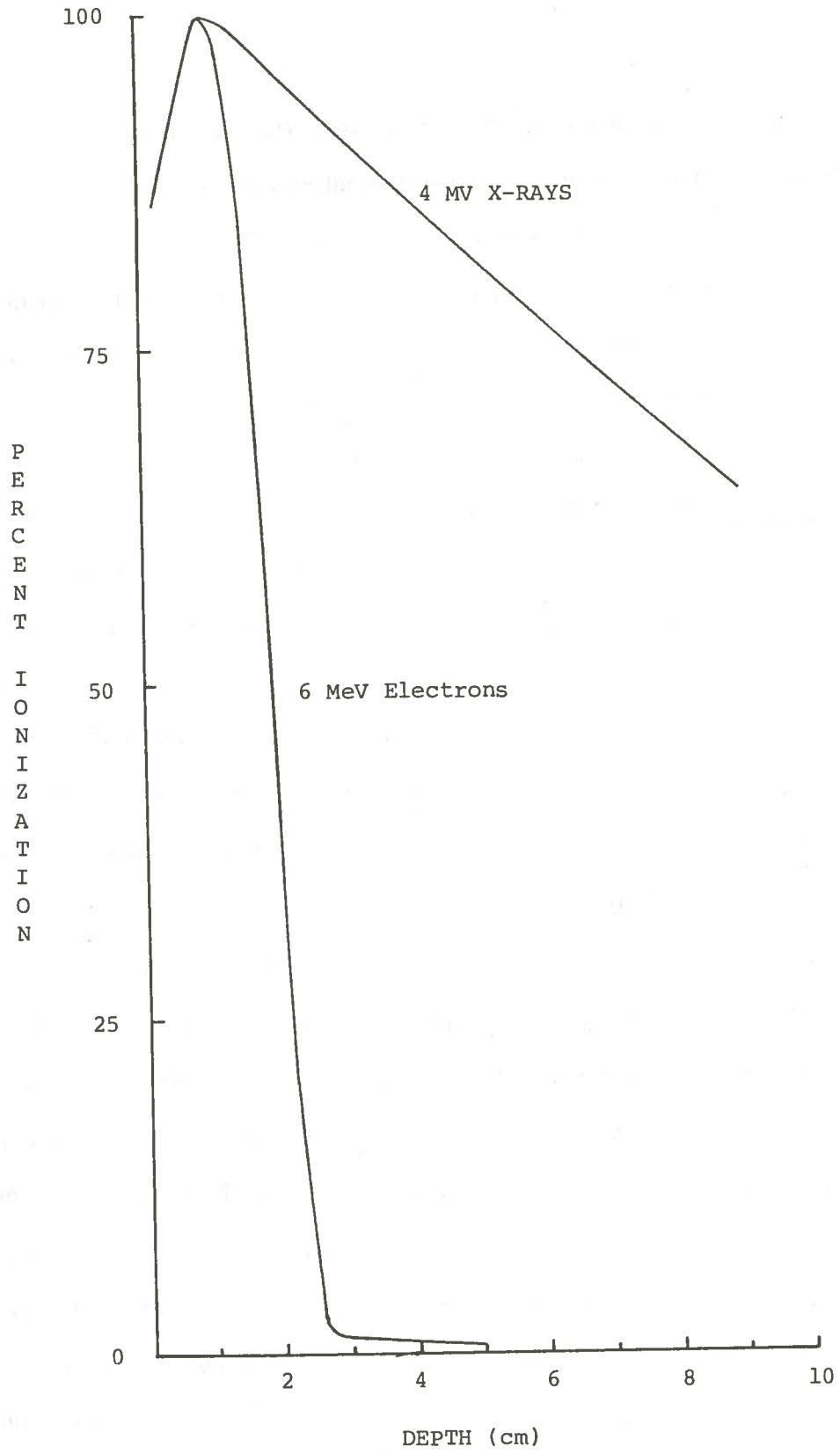

Fig. 1. Comparison of depth ionization curves for a 6 MeV electron beam and 4 MV x-rays.

prescribed dose, then adequate dose uniformity is presumed to occur and the penetrability of the beam is similarly presumed to be sufficient without unduly affecting deeper tissues. The selection of electron beam energy is determined with respect to the beam measured at the surface of the patient. Variations in technique, geometry and the mass of the material in the beam, all determine the electron energy at the surface of the patient. The ionization measured at different depths in a phantom, when plotted against the depth at which the ionizations occurred, yield curves characteristic of electron beams. As measurements are taken at ever greater depths, the relative measured ionization decreases rapidly until finally a small plateau is reached which further decreases only slightly with depth.

When high-energy electrons pass through a condensed medium, they undergo radiative interactions, including ineleastic collisions. In this instance, an electron passing close to the nucleus of an atom is attracted by its large positive coulombic charge, causing it to undergo a change in angular momentum. When the electron leaves the vicinity of the nucleus, it does so with less energy than when it entered. The difference in energy is converted to an electromagnetic photon called bremsstrahlung. Electron beams, therefore, are always accompanied by such photon contamination which is called bremsstrahlung (a German word meaning "braking-radiation") or x-rays. (In this thesis, these two terms are used interchangeably.) The amount of bremsstrahlung contamination in the electron beam varies with the accelerator operating conditions.[1,2] The contribution to the beam is generally considered to be less than 5% of the maximum electron dose.[3,4]

The tolerance of the body to ionizing radiation depends on the energy deposited in the tissue and the length of time during which it is deposited. When

the dose is fractionated over a period of weeks, the effects are generally less severe than if the dose is received all at once. If the x-ray component of the treatment cumulatively totaled to 100 rads, (less than 3% of the average dose) it could very well be dose-limiting if the bone marrow activity showed signs of being suppressed.[5] The patients' blood counts are checked frequently and the radiation is monitored carefully because the response of the individual, who is already in a reduce state of health, cannot be forecast with certainty.

Although bremsstrahlung is an inevitable problematic component of an electron beam, techniques can be applied to minimize them. The method of administering electron beam irradiation of the total skin surface at the Mary Bird Perkins Radiation Treatment Center in Baton Rouge, Louisiana follows, somewhat the Stanford technique, which was described by Karzmark.[2,3,6] In this technique, the patient is placed approximately 10 feet from the radiation source, and the irradiations are made with the patient in six different orientations (see Figure 2). At each orientation, the electron beam is angled first 20 degrees above and then 20 degrees below the horizontal, for a total of twelve treatment positions. The raising or lowering of the beam by 20 degrees is done to achieve dose uniformity across the surface of the patient. Karzmark[3,7] has stated that the x-ray component accompanying the primary electron beam apparently occupies a relatively narrow forward angle in the center of the beam. Hence, with the beam angled above or below the patient, the x-rays are directed outside the patient treatment volume.

Since the linear accelerator and the physical facilities at the Perkins Radiation Center vary from those used at Stanford University, and since we know that the amount of bremsstrahlung produced is dependent on the accelerator operating conditions, it is necessary to evaluate the contaminating

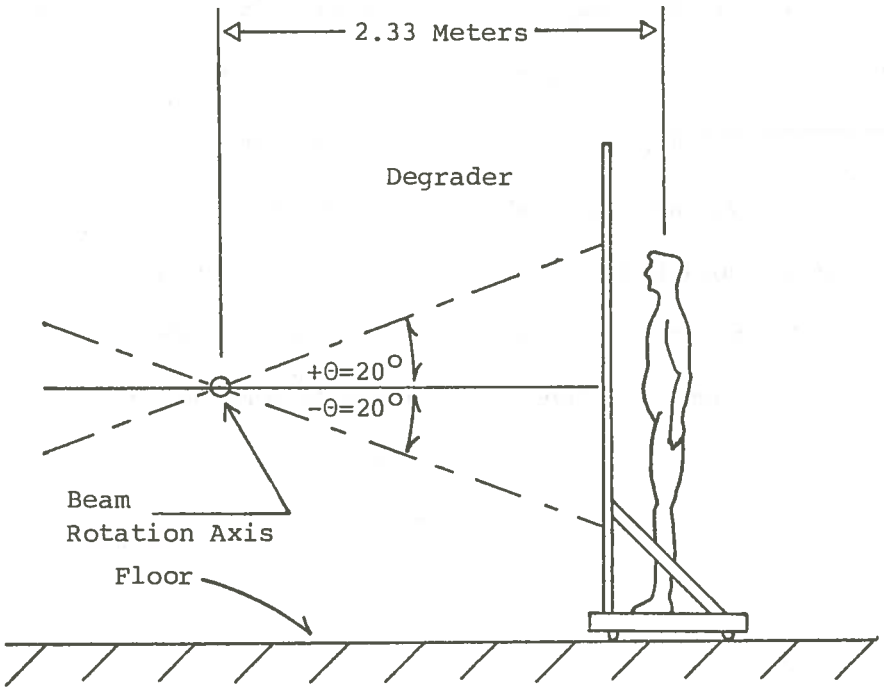

Fig. 2. Patient treatment position for 100 cm SSD linear accelerator. Total treatment distance, including 100 cm center of rotation equals 333 cm. Six patient orientations are treated, each with $+20^{\circ}$ and -20°; AP, PA, Right Anterior Oblique, Left Anterior Oblique, Right Posterior Oblique, and Left Posterior Oblique.

bremsstrahlung component of the electron beam to insure the patency of the prescribed treatment.

It is the purpose of this thesis, therefore, to demonstrate the effect that changing the treatment geometry has on the percentage of bremsstrahlung present as measured by ionization chambers. Determination of the dose which the bremsstrahlung may contribute to the overall treatment of the patient, is not the aim of this study. It is theorized that the x-ray radiation present in the treatment field accounts for a small though measureable percentage of the total radiation present. It is expected that the systematic evaluation of each geometric change from standard positioning to the modified Stanford technique, will reveal the most favorable combination of treatment parameters, that is to say, the geometry in which the bremsstrahlung component is as small as possible.

METHODS AND MATERIALS

The Varian Clinac 18 linear accelerator at Mary Bird Perkins Radiation Treatment Center is capable of producing 10 MV x-rays and 6, 9, 12, 15 and 18 MeV electron beams. Since all of these radiation energies are more penetrating than are desired for the treatment of mycosis fungoides it is necessary to reduce the energy of the radiation delivered to the patient. A 6 mm thick sheet of polystyrene reduces the energy of the 6 MeV electron beam to approximately 4 MeV.[8] Collimating and degrading the electron beam creates a significant clinical problem by producing bremsstrahlung. Bremsstrahlung must therefore be considered in designing the electron treatment plan.

The technique used for electron irradiation of the total skin is a modification of techniques used elsewhere.[2,3,6,9] At Perkins Radiation Center, a portable energy degrader consisting of polystyrene screen 1 meter wide by 2.2 meters high, 6 mm thick is positioned three meters from the source of radiation. Patients are treated by standing behind this screen while 6 MeV electrons are beamed through the screen at an angle of 20 degrees above and below the horizontal (see Figure 2). This angulation distributes the overall electron dose more evenly on the vertical axis. For the purposes of evaluating patient doses, measurements are taken at the patient treatment position.

To evaluate the bremsstrahlung contamination, it was first necessary to calibrate the measuring equipment under known conditions. A PTW Markus parallel-plate ion chamber was available for use in this study, and it was decided to compare it to the calibrated PTW Farmer-type ion chamber under standardized conditions used to calibrate the accelerator. The ion chambers

were used in conjunction with a Keithley electrometer, to collect positive or negative charges (coulombs).

Once the calibrated Farmer-type ion chamber was irradiated in a standard accelerator geometry, the Markus parallel plate ion chamber was then substituted for the Farmer chamber. Small parallel plate ion chambers have several distinct advantages for use in evaluating low energy electron beams.[4,7,10,12,13] These advantages include an effective point of measurement virtually at the surface of the chamber, no significant perturbation correction, and less sensitivity to backscatter variations at low electron energies. Parallel plate chambers also have small volumes and recombination of ion pairs at normal operating voltages does not appear to be a problem.[11] The supporting data supplied with the Markus chamber indicates that at collecting potentials between 300 and 400 volts (where our data was taken) greater than 99% ion collection is achieved. These characteristics, coupled with the small chamber volume (0.04 cc), made the Markus chamber ideal for measuring the ionization occurring at specific depths within the water phantom.

The subsequent data were collected changing one characteristic of the geometry for each set of data gathered. This procedure allows the determination of the cause of changes in the depth ionization curve and its bremsstrahlung tail. The measurements were taken with the beam perpendicular to the face of the phantom. All ionization readings were corrected for temperature and pressure variations to 22°C and 760 mm Hg. The Varian procedures call for a collimator setting of 15 x 15 cm for the 10 x 10 cm cone and this was used. Readings were made on both positive and negative polarities. The readings so obtained were averaged by subtracting the negative polarity

reading from the reading obtained on the positive polarity and dividing the sum by two.[14]

The first of these measurements was taken at a standard 100 cm source to skin distance for a 10 x 10 cm field such as is used in calibration of the linear accelerator as shown in Figure 3. The Farmer-type, 0.6 cc cylindrical ion chamber was utilized for these measurements. The chamber was irradiated in a 41 x 41 x 38 cm plastic water phantom equipped with a 20 x 20 cm window that is 1.5 mm thick. The ion chamber was attached to a Keithly Model #616/6169 electrometer and biased with a 337.5 volt potential. The readings obtained in this configuration were comparable with those obtained during accelerator calibrations.

After the first set of measurements, the 10 x 10 cm cone was removed, then, the collimators were opened from 15 x 15 cm to 36 x 36 cm. The effect of placing a small 6 mm thick polystyrene plate over the collimator aperture was then evaluated. This was done because the patients are given supplemental irradiation to low dose areas using this method of degrading the beam. This was also done to compare the effects of positioning the polystyrene degrader at the treatment head as opposed to its being near the patient.

Another series of measurements were made at a distance approximating a normal treatment geometry. The phantom was centered on the central axis of the horizontal beam at a total treatment distance of 333 cm. Depth-ionization data were collected under these conditions with and without the polystyrene sheet at the treatment head. Then the full degrader was positioned at 300 cm with the phantom remaining in the same relative position (see Fig. 4).

Finally, the last step in approximating a treatment position was made. The incident beam was angled 20 degrees, first above and then below the

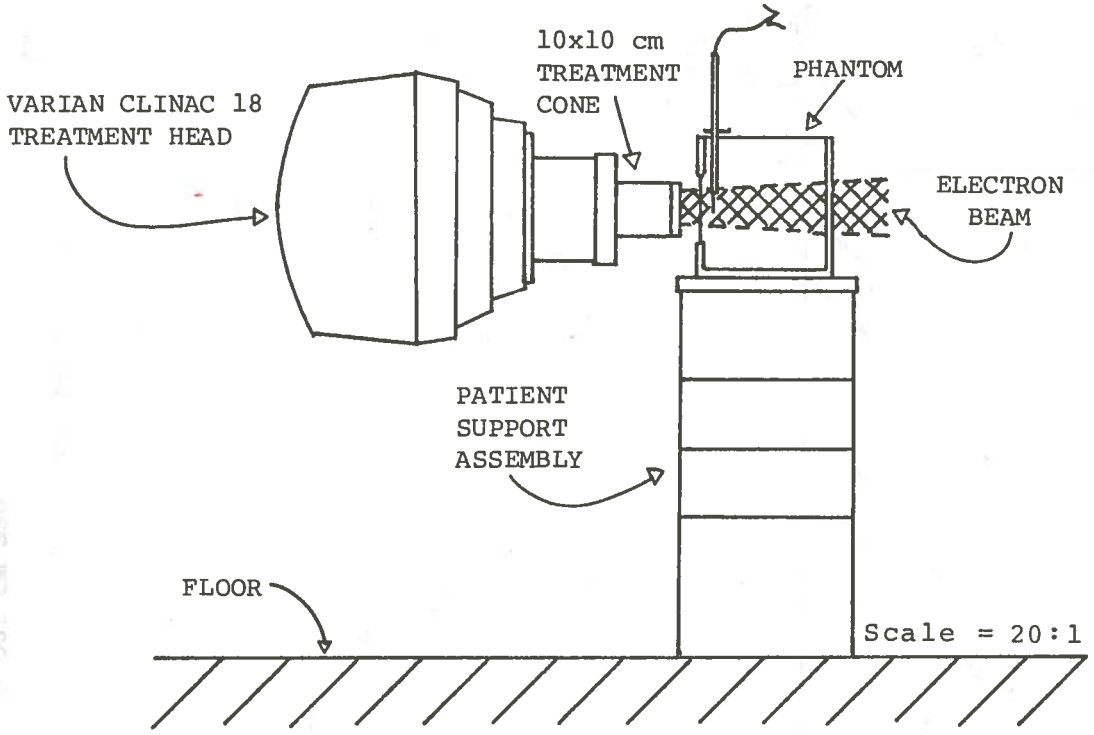

Fig. 3 Calibration geometry for electron beams. The beam is directed horizontally (270°) into the water phantom containing the ion chamber. The source-to-surface (SSD) distance is 100 cm.

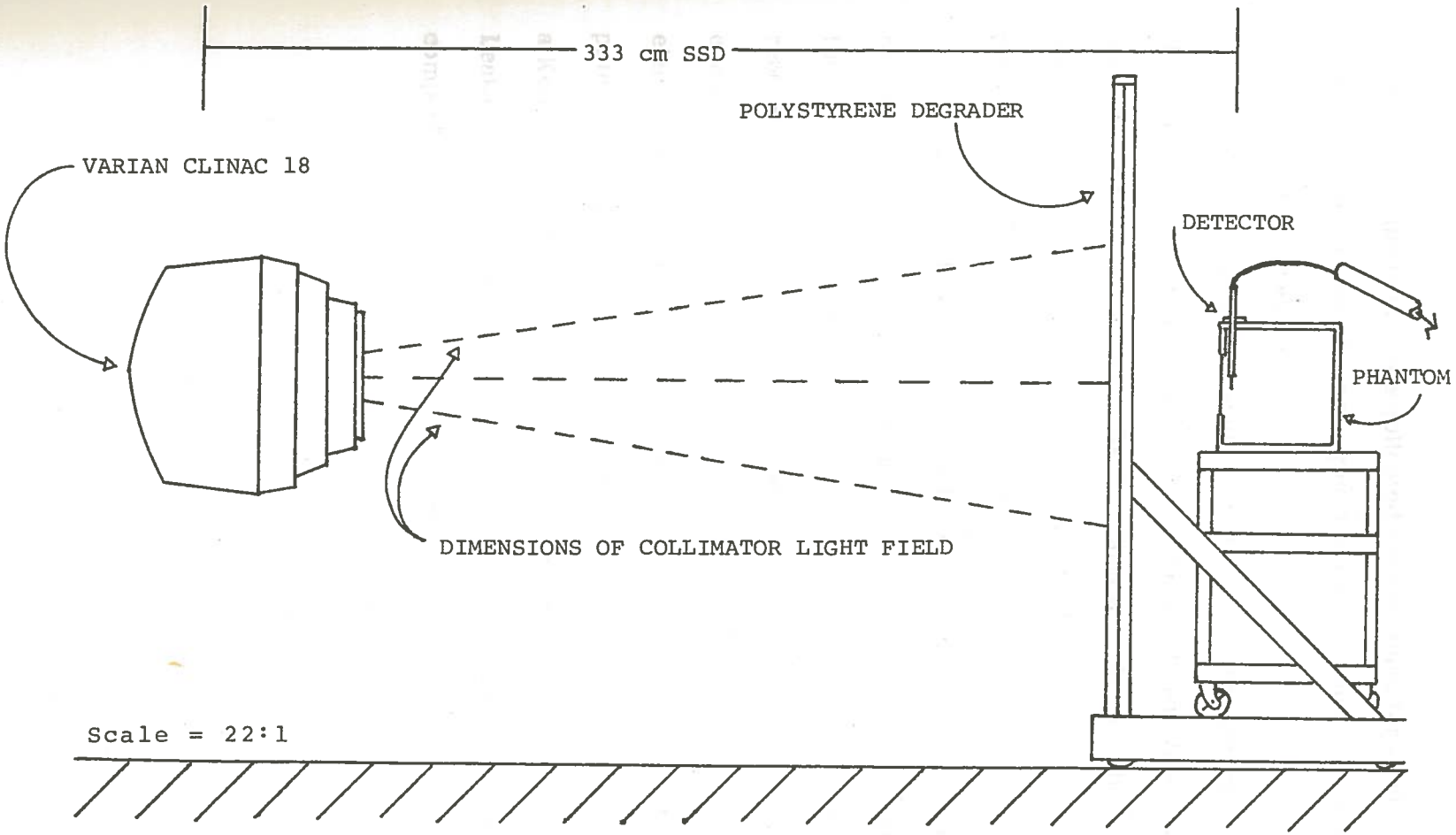

Fig. 4. Measurement geometry at 333 cm SSD. Collimator setting is 36x36 cm field size. The ion chamber is positioned in line with the central axis of the radiation field. The polystyrene degrading screen may be removed for certain measurements, however, the relative positions of the electron beam, the phantom, and the ion chamber remain unchanged.

horizontal and the ionizations collected were summed for each depth (see Fig. 5). This procedure allowed for averaging the electron and photon ionizations taken at mid-line in the phantom.

Due to the 20 degree angling of the beam, the position of the detector at the center of the phantom lies outside the treatment field as defined by the accelerator's collimator light field. However, due to the broadening of an electron beam by scatter and charge effects the mid-line of the phantom is probably well within the electron field.

Stem effect, that is, the radiation effect on the connecting cable, was reduced or eliminated in large fields by the use of galvanized steel piping through which the connecting cables were routed. Each geometry was reproduced several times and the relative numbers obtained were cross-compared among chambers and among different electrometers. The electrometers used included a Keithley Model 602 with the ion collecting potential supplied by a 300 volt battery. A Keithley Model 615 electrometer and a Keithley 616 electrometer were utilized to measure the total charge collected. Leakage current was very small and offset using the "background" circuit to compensate for any instrument drift encountered.

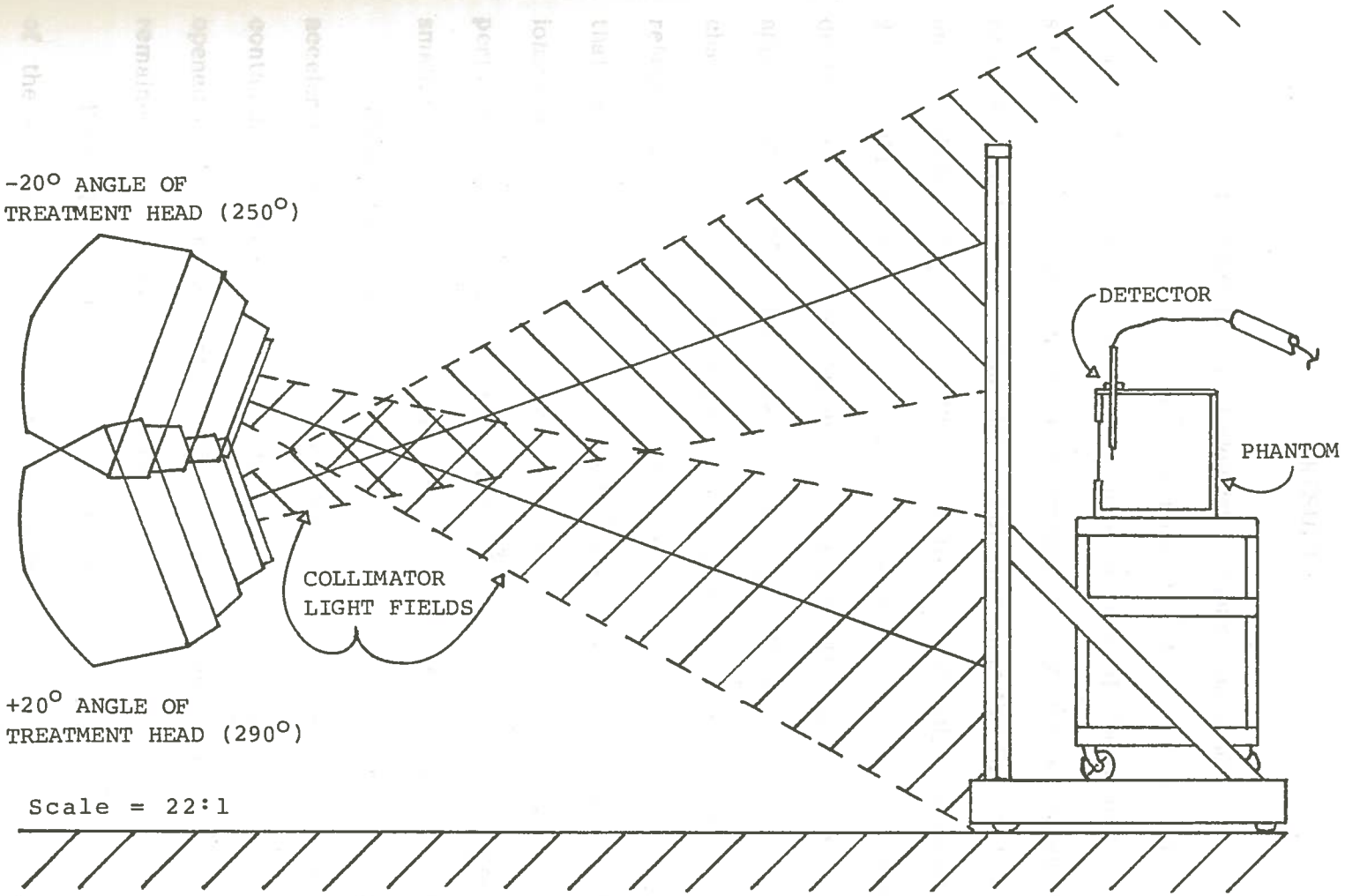

Fig. 5. Final measurement geometry at 333 cm SSD. The treatment head is alternately angled 20° above and below the horizontal. Bremsstrahlung is directed away from the detector using this technique which also produces a more uniform electron distribution along the vertical axis in the plane of the beams.

RESULTS

The data described in following sections and which are plotted in a number of figures, have all been normalized to the ionization at D_{max}. The relative depth ionization curves for each geometrical change to the irradiation setup have been plotted in Figures 6 through 12. Figure 6 is a comparison of the relative ionizations at various depths obtained using the Farmer-type chamber and the Markus chamber in a 10 x 10 cm field and at 100 cm as shown in Figure 2. With this geometry, it is shown that the "tail" on the curve beyond 2.8 cm depth represents the photon contamination of this beam which amounts to approximately 0.8% of the ionization at D_{max}. When the Markus parallel plate chamber was substituted for the Farmer chamber in the same geometry and the relative ionization referenced to the same depths in the phantom, it was found that the Markus chamber also yielded bremsstrahlung amounting to 0.8% of the ionization at D_{max}. It has been stated that with parallel plate ion chambers, perturbation corrections can be ignored.[12] Since perturbation corrections are small, their influence on this small percentage cannot be confirmed or denied.

When the 10 x 10 cm electron beam cone was removed from the accelerator and the collimators were left at 15 x 15 cm, the amount of photon contamination decreased only slightly to 0.75%. When the collimators were opened to their full capacity of 36 x 36 cm, the bremsstrahlung contamination remained unchanged at 0.75% (see Figure 7).

Figure 8 shows that with the addition of 6 mm polystyrene sheet in front of the collimator aperture, the bremsstrahlung increased to 1.0% of the ionization measured at D_{max}.

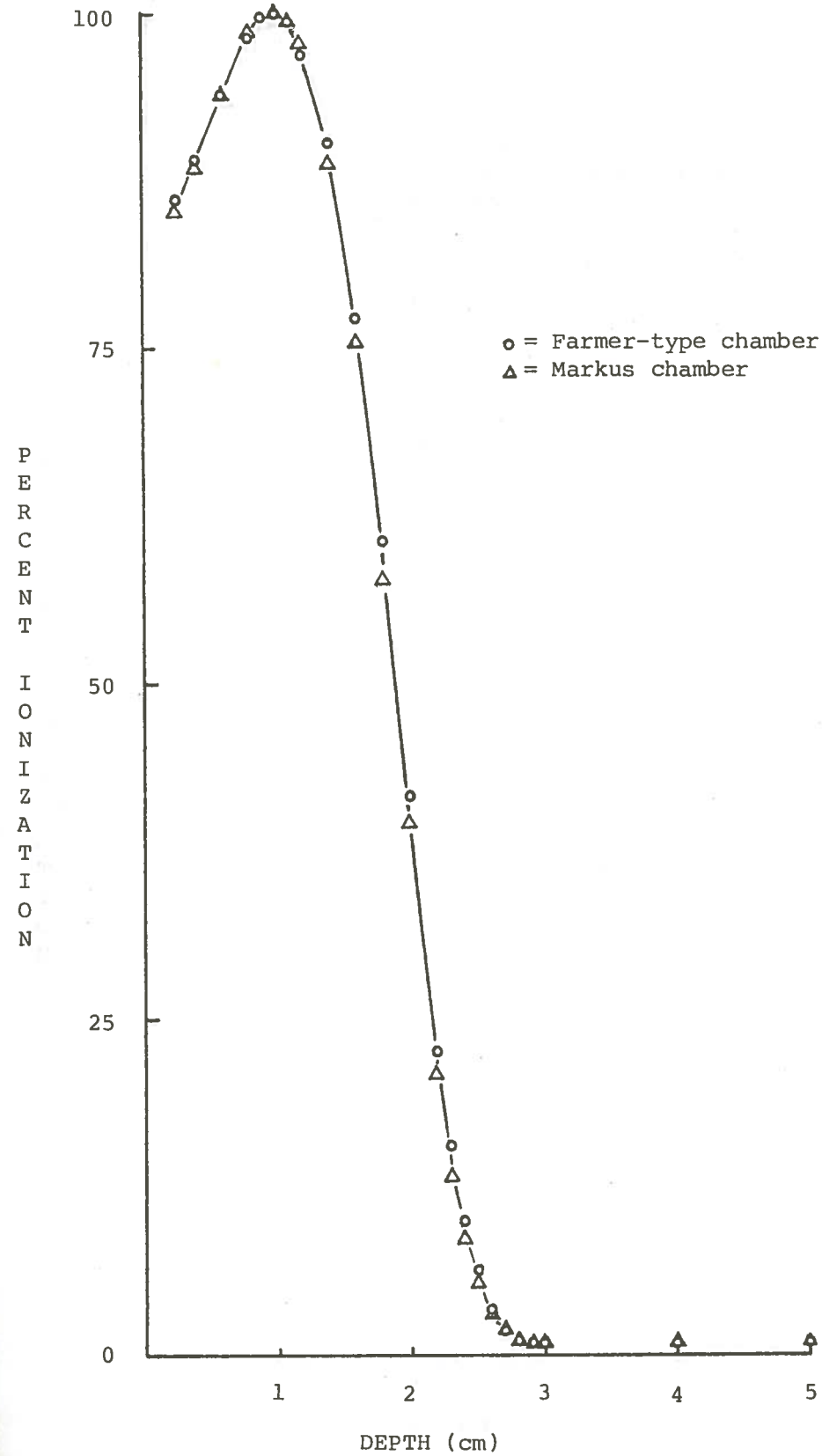

Fig. 6. Comparison of the ionization produced in a water phantom as measured a nylon Farmer-type cylindrical ion chamber and a Markus lucite parallel-plate ion chamber.

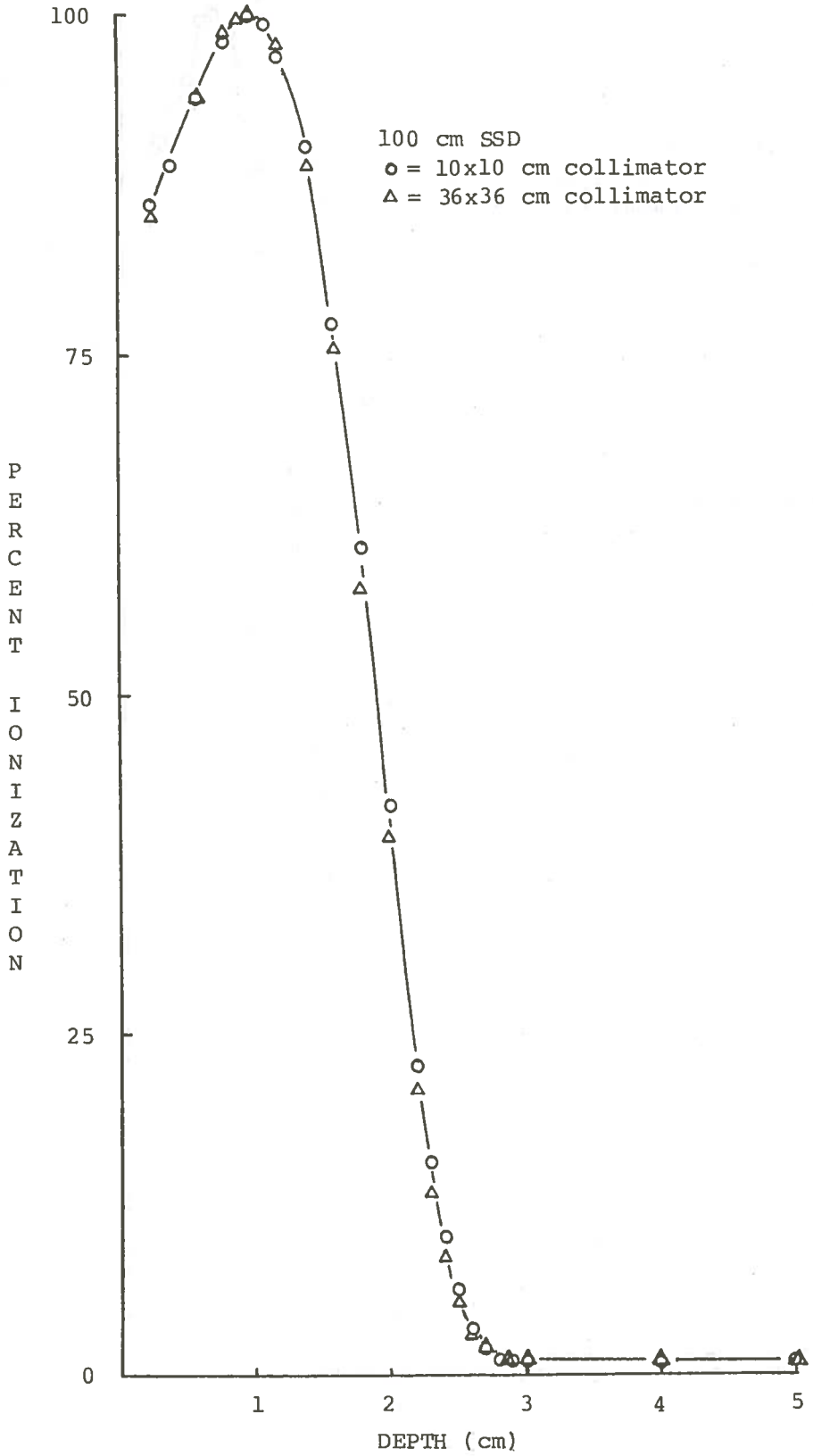

Fig. 7. Comparison of 10x10 cm and 36x36 cm field sizes at 100 cm SSD.

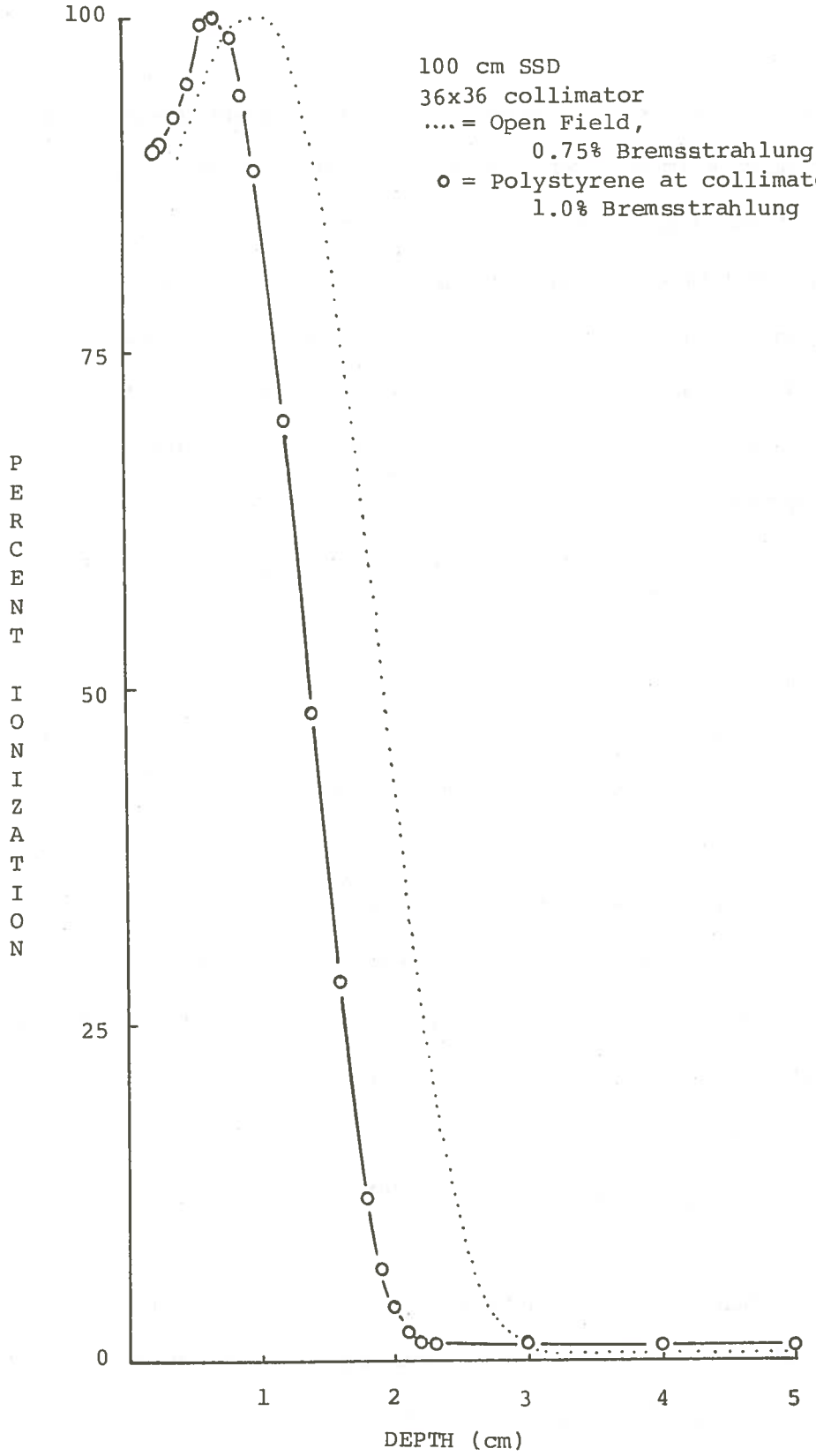

Fig. 8. Demonstration of the change in relative ionization curves resulting fron the placement of polystyrene over the collimator aperture, and the consequent increase in x-rays.

At the treatment distance of 333 cm, ionization measurements without the degrader in place were made with the open beam perpendicular to the window of the phantom (see Figure 3). The result, as shown in Figure 9, is that the bremsstrahlung radiation increased to approximately 1.7% of the ionization at D_{max} as a result of the longer air column. The addition of the 6 mm polystyrene sheet to the collimator opening made the most dramatic change on the percentage contribution of bremsstrahlung observed throughout the experiment. Figure 10 shows that the previous amount of x-ray contamination observed more than doubled to a total of 3.6% of the D_{max} ionization.

The next step involved placing the 6 mm of portable polystyrene degrader in a position near the detector. The degrader was placed at 300 centimeters source-to-surface distance (SSD) with the phantom remaining at 333 centimeters. Here the bremsstrahlung contamination dropped from the previous reading to the level of 2.3% of D_{max} (see Figure 10). In other words, the movement of the polystyrene from near the source to near the detector reduced the effective x-ray contamination to two-thirds of its previous value.

In the last geometric arrangement (see Figure 4) the treatment field is angled 20 degrees above and below the horizontal. The edges of the light fields from the accelerator indicate that there is about a 40 cm gap between the beams at the position of the degrader. Ionization measurements here did not confirm the presence of bremsstrahlung. This situation is discussed in greater detail in the following sections. Figure 11 is a diagram of the percent ionization for the 20 degree up and 20 degree down angulations as well as the sum of both. Figure 12 is a comparison of the relative levels of photon contamination in each configuration described above.

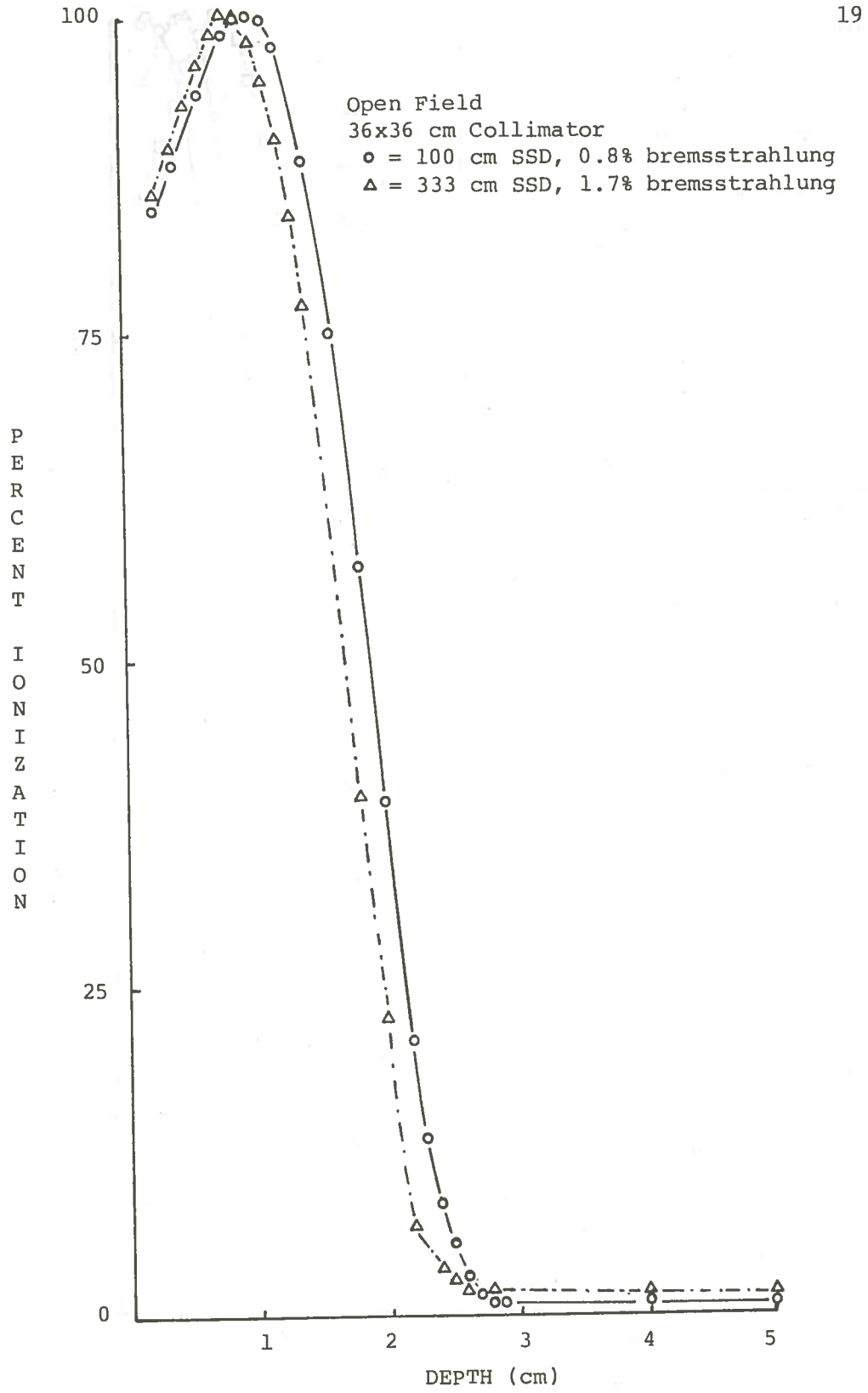

Fig. 9. Demonstration of the change in percentage photon contamination as a result of increasing SSD.

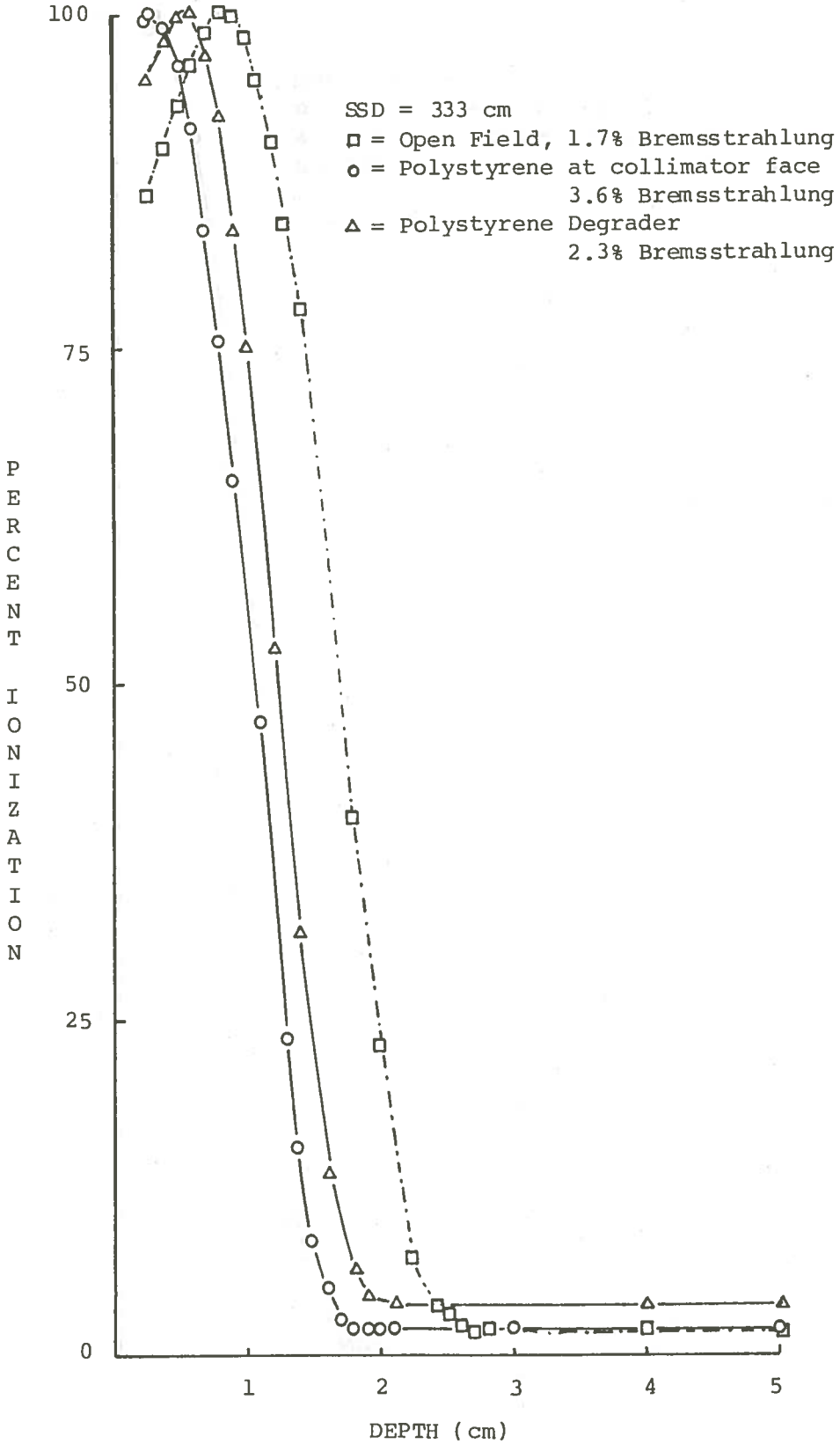

Fig. 10. Demonstration of the effects of positioning the degrading material at different location relative to the non-degraded beam.

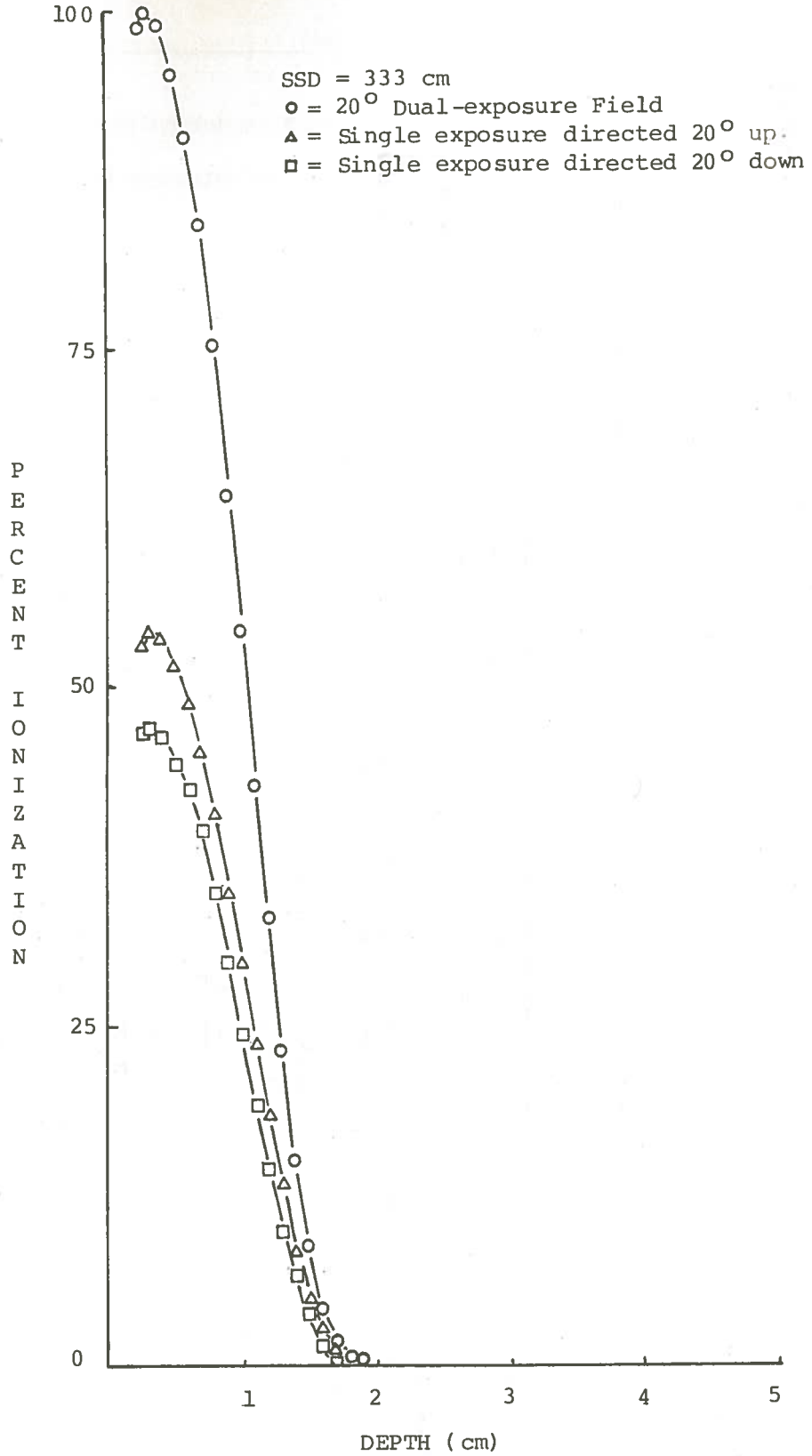

Fig. 11. Demonstration of the single exposures and the composite 20° dual-exposure field.

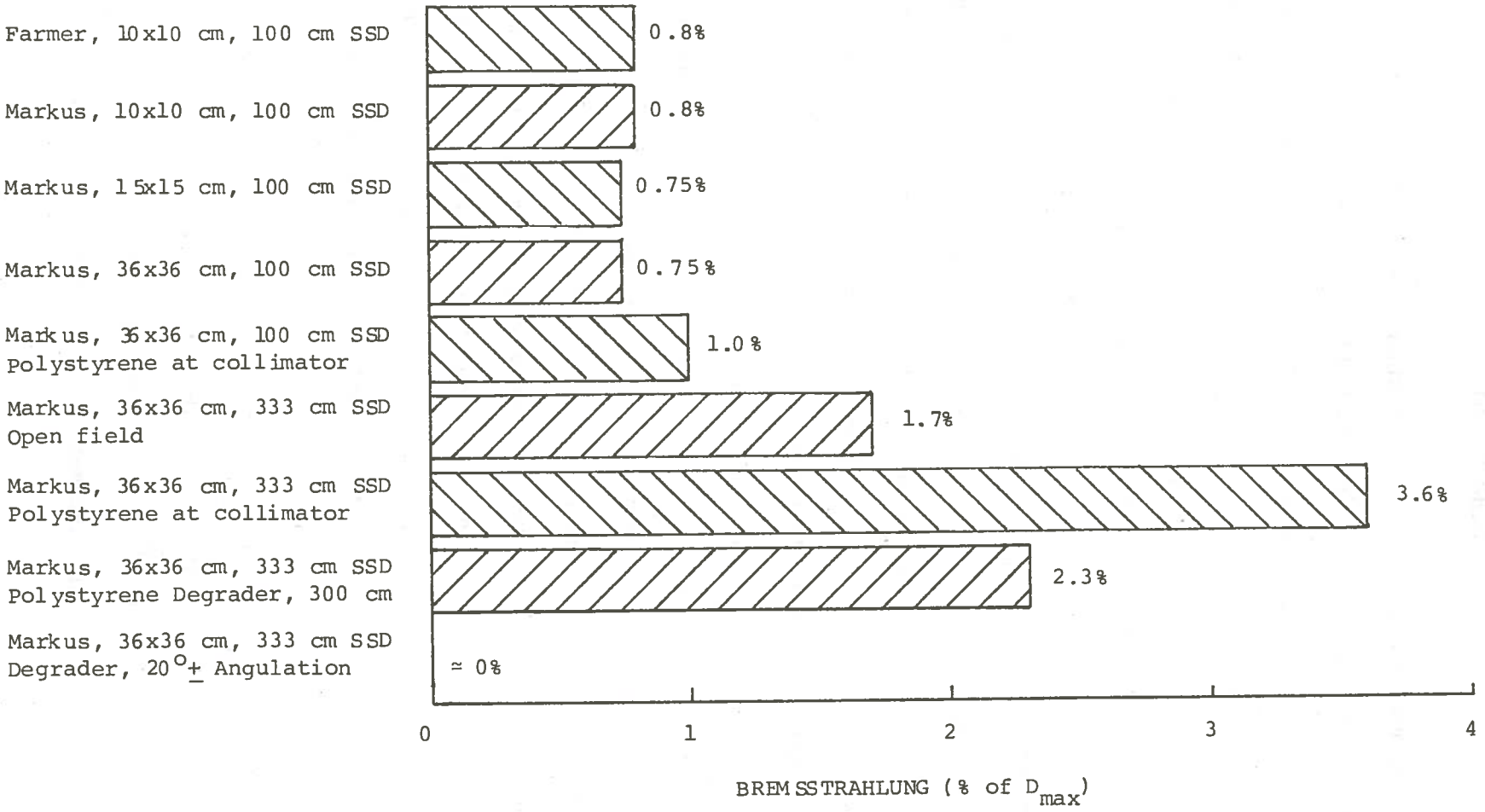

Fig. 12. Percentages of bremsstrahlung contamination as a function of the maximum ionization measured for each geometry.

DISCUSSION

When the data are normalized, the relative ionization versus depth plotted in Figure 6 yields virtually identical curves for the Farmer and the Markus ionization chambers. Figures 6 and 7, representing the data taken at 100 cm, show little variation with the exception of the build-up region, which does not really concern the subject of this study. In all probability, the variations seen in the build-up region are due, at least in part, to different sensitivities of the two ion chambers to in-scatter and back-scatter due to their inherent variations in design, as well as varying energies of electrons scattered into the phantom surface. The relative amount of bremsstrahlung observed at the 100 cm distance appears to be fairly constant with a slight decrease noticed after the 10 x 10 cm cone is removed. Since this cone contains a thick aluminum border which serves to define the electron beam, it is probable that the decrease in bremsstrahlung is a result of decreased electron interactions with the metal of the cone. The removal of this cone removes a very small fraction of the bremsstrahlung which constitutes the difference seen in Figure 12. The remainder of the bremsstrahlung detected is in all probability due to axial components in the beam (i.e., accelerator window, scattering foil, and transmission ionization chamber). Since there is virtually no difference in the bremsstrahlung observed with the collimators set at 15 x 15 cm and 36 x 36 cm, it is assumed that the collimators do not play an important role in the production of contaminating x-rays.

When the 6 mm sheet of polystyrene is placed across the collimator opening, a definite rise in the bremsstrahlung relative to D_{max} is noted. However the total charge collected by the electrometers in each of these instances amounts to approximately 0.3×10^{-10} coulombs per 200 monitor units, at 4 cm depth in the phantom. Consequently, it appears not that the x-rays are

being increased due to interactions in the presence of the polystyrene, but that the number of electrons contributing to D_{max} is being reduced in the polystyrene by absorbtion and scatter. The total x-ray portion of the beam remains relatively constant.

When the phantom is moved to the treatment position of 333 cm, a curve is produced (see Figure 9) which indicates a beam of slightly reduced energy and of slightly increased photon component. The cause of this change is due to the same basic phenomena seen with the polystyrene at 100 cm. Instead of polystyrene, the additional large air volume traversed increases the number of electrons scattered out of the beam. Additionally, due to the inverse square effect, the electron fluence is reduced by approximately a factor of 10. Consequently, the overall increase in bremsstrahlung as a function of D_{max} is much greater, amounting to over a 50% increase above what was seen with the polystyrene at 100 cm SSD (1.7% of D_{max} ionization).

When the polystyrene was placed at the accelerator head, a dramatic increase in x-ray contamination was observed at the 333 cm SSD. The polystyrene at the treatment head serves to scatter and absorb a great many electrons from the beam with the net effect of greatly reducing the electron flux. Therefore, the resulting bremsstrahlung contamination becomes a 3.6% component of the treatment beam. This scattering and absorption of electrons may be assumed since the electrometer readings recorded within the bremsstrahlung tail under both geometries were approximately equal at 0.4×10^{-11} coulombs per 200 monitor units.

When the normal treatment position is used with the gantry angled 20° up and 20° down from the horizontal, bremsstrahlung at a distance just beyond the practical range also measures approximately 0.4×10^{-11} coulombs. However,

since the bremsstrahlung tail cannot be well demonstrated with the data collected in this configuration, it is possible that the readings just beyond the practical range are due to electrons giving up the last of their energy. Since the gantry is angled, it would be expected that the photon component of the beam would be missing the ionization chamber to a great extent. The small volume of the Markus chamber and the depth of the phantom combined to give extremely small numbers which may be approximating the level of electronic noise within the cable. The experimental procedure may need to be modified to utilize the calibrated Farmer type ionization chamber at these depths in order to quantify more precisely the bremsstrahlung component (See Appendix). It is assumed that most of the photon contamination is directed above and below the patient and is therefore not detected at the midline measuring point chosen for this study.

CONCLUSIONS

The Farmer-type thimble ionization chamber was compared with the Markus parallel plate ionization chamber. The effective point of measurement of the Farmer chamber was taken to be 3/4 of the radius of the thimble back toward the source of radiation as widely discussed in the literature concerning electron beam dosimetry. The effective point of measurement of the Markus chamber is considered to be the front plate. When these offsets are considered and the relative ionizations corrected for inverse square effects, the data graphed in Figure 6 are virtually identical, including the levels in the bremsstrahlung "tail" of the curve. These values amounted to 0.8% of D_{max} in both instances. It is apparent from this comparison that the Markus chamber compares favorably with the Farmer chamber.

When the electron beam treatment cone was removed and measurements were made with the collimators set at 15 x 15 cm and 36 x 36 cm, the result was that the total ionization observed at D_{max} increased by almost 20% (3.64×10^{-9} vs 4.32×10^{-9} Coulombs per 200 monitor units). However, the percentage of bremsstrahlung radiation observed decreased from the 10 x 10 cm value slightly to 0.75% at 15 x 15 cm and it remained constant at 0.75% even with the collimators opened fully. This finding indicates that the removal of the 10 x 10 cm cone which has a large metal defining frame at its base, increases the available number of electrons that may scatter to the phantom. However, the bremsstrahlung that is produced from axial components within the beam and that which is scattered from the collimating surfaces of the treatment head are not dependent upon the individual collimator settings and it is merely a function of the total radiation emitted.

The addition of 6 mm of polystyrene over the collimator aperture resulted in an obvious and expected displacement of the curve towards the lower values (see Figure 8). The energy of the incident beam on the phantom is decreased as evidenced by the reduced practical range, which is determined by the intercept of the steepest portion of the curve with the extrapolated bremsstrahlung plateau.[15,16,17] The polystyrene also caused a reduction of the total ionization at D_{max} by slightly more than one-third. This is indicative of a significant portion of the electron beam being absorbed or scattered and thus never reaching the phantom. This phenomenon resulted in a corresponding increase in the percentage of bremsstrahlung relative to D_{max} by about one-third to one percent. Therefore, it may be concluded that the addition of polystyrene does not contribute in any meaningful way to the increase in bremsstrahlung but it does significantly reduce the total ionization at the phantom surface by greatly reducing the flux of electrons.

At the treatment distance of 333 cm, ionization measurements were made with the open beam perpendicular to the front of the phantom. By relocating the phantom to the treatment distance, the electron beam must traverse a much greater air volume. Of course, there is also the inverse square effect, which would be expected, independent of other effects, to reduce the incident flux to approximately 15% of the value at 100 cm. Since electrons are very readily scattered even in air, it is not surprising that the measured D_{max} values dropped by more than 15% to less than 7% of the value at 100 cm SSD. However, the bremsstrahlung "tail" decreased to approximately 14% of the value at 100 cm SSD thereby resulting in a net increase in the bremsstrahlung to 1.7% of the ionization seen at D_{max}.

When the measurements taken on the unrestricted electron beam at 333 cm are compared to the same beam with 6 mm of polystyrene placed over the collimator aperture, the most dramatic change in the entire series is observed (see Figure 10). D_{max} of the ionization curve is reduced to less than 40% of that without the polystyrene sheet. Meanwhile the bremsstrahlung radiation is reduced to 85% of its unrestricted value without the polystyrene sheet. It may be concluded that placing the polystyrene at the head of the accelerator has the effect of increasing the bremsstrahlung relative to D_{max}. In this configuration the increase amounted to 3.6% of D_{max}.

When the polystyrene is placed as shown in Figure 4 with the degrader located at 3 meters from the source, the effects are quite different. First, the ionization at D_{max} is only reduced to about 92% of the value in the beam without the degrader present. By placing the degrader close to the phantom surface, the electrons scattered by the degrader are less likely to have been scattered out of the beam, than when they are scattered early in the track length. Secondly, the bremsstrahlung portion of the curve is virtually identical to the same portion of the unrestricted beam curve, except that the degraded beam curve is naturally displaced towards the origin somewhat as would be expected with a less energetic beam at the detector. Since the bremsstrahlung is unchanged, it may be concluded that it is arising in the head of the accelerator, not in the polystyrene.

The final data were collected in a manner differing from those collected previously as noted in Figure 5. In this situation, the treatment beam being measured is angled 20 degrees above and below the horizontal. The phantom and ion chamber are located outside of the line-of-sight borders of the radiation field. However, the coulombic effects of an electron beam tend to force the

beam to expand beyond its collimated borders.[18] The beam is also scattered and degraded by the air and polystyrene. Therefore, the ion chamber is located in a low flux area, midway between the central axes of these beams.

Since the central axis of the beam is now directed alternately above and below the detector, it would be expected that the x-ray contamination at the midline of the phantom would be a very small component, if present at all. It was found that somewhat more electron scatter was evident when the beam was angled toward the floor than when it was angled above the degrader (see Figure 11). This finding presumably was due either to the more efficient scattering off of concrete flooring than from air and a more distant concrete ceiling or residual stem effect in that portion of the cable which could not be shielded. The use of the Markus parallel plate chamber with its 0.04 cc volume does not generate a very large signal for the electrometer to read. Regardless of this fact, no significant readings could be obtained at depths beyond 1.9 cm, and no bremsstrahlung was evident. The use of the Farmer type chamber with its 0.6 cc volume and a concomitantly higher signal is able to demonstrate the bremsstrahlung at levels below which the Markus chamber is insensitive (see Appendix).

The most striking finding of this series of step-wise measurements is that the mid-line contribution of bremsstrahlung to total ionization under this treatment regimen is too small to be measured with the Markus ionization chamber. Therefore, at least in this series of points measured in the phantom, x-ray contamination is probably less than 2%. It will be reasonable to assume that this may not remain true if the phantom is moved cephalad and caudad from the position used in this geometry.

It is apparent that in the treatment of mycosis fungoides using low energy electron beams, the most important factors are angling the beam to achieve uniformity without the central axis being directed towards the patient and the positioning of the degrader near the patient rather than making it part of the treatment head.

REFERENCES

1 J. Spira, C. Botstein, B. Eisenberg, and W. Berdon, Am. J. Roentgenol. **88**, 262 (1962).

2 C. J. Karzmark, Br. J. Radiol. **37**, 436 (1964).

3 C. J. Karzmark, R. Loevinger, and M. Weissbluth, Radiology **74**, 633 (1966).

4 S. C. Klevenhagen, G. D. Lambert, and A. Arbabi, Phys. Med. Biol. **27**, 363 (1982).

5 P. Rubin and G. W. Cassarett, Clinical Radiation Pathology, Vol II, (Saunders, Philadelphia, 1976). pp. 808-813.

6 V. Page, A. Gardner, and C. J. Karzmark, Radiology **94**, 635 (1970).

7 W. F. Hanson, L. W. Berkley, Med. Phys. **9**, 607 (1982) (abstract).

8 W. S. Kubricht (personal communication).

9 L. Z. Nisce, G. J. D'Angio, and J. H. Kim, Radiology **109**, 683 (1973).

10 AAPM Report of Task Group 21, A protocol for the determination of absorbed dose from high energy photon and electron beams (American Institute of Physics, New York, N.Y., 1983)

11 Recommendations by the Nordic Association of Clinical Physics (NACP) 1980, Procedures in external radiation therapy dosimetry with electron and photon beams with maximum energies between 1 and 50 MeV, Acta Radiol. Oncol. **19** (1980) Fasc. 1.

12 Supplement to the Recommendations by the Nordic Association of Clinical Physics (NACP) 1980, Electron beams with mean energies at the phantom surface below 15 MeV, Acta Radiol. Oncol. **20** (1981) Fasc. 6.

13 H. Svenson and G. Hettinger, Acta Radiol. Ther. Phys. Biol. **10**, 369 (1971).

14 K. Hogstrom (personal communication).

15 ICRU Report No. 21, Radiation dosimetry: Electrons with initial energies between 1 and 50 MeV (ICRU, Washington, D.C., 1971).

16 N. Suntharalingam, "Dosimetry of Electron Beams," in Practical Aspects of Electron Beam Treatment Planning, AAPM Monograph No. 2 (American Institute of Physics, New York, 1978).

[17] P. R. Almond, "Radiation Physics of Electron Beams," in Clinical Applications of the Electron Beam, edited by N. duV. Tapley (Wiley, New York, 1976).

[18] SCRAD Committee of AAPM, Protocol for the dosimetry of high energy electrons, Phys. Med. Biol. 11, 505 (1966).

APPENDIX

Preliminary Dosimetry Calculations

A natural continuation of this thesis is to determine the dose to a hypothetical patient undergoing the treatment described for mycosis fungoides. A dose determination was made at the same relative position as utilized in the final geometry (see Figure 5). The only change to this geometry was that a Farmer-type ion chamber was placed at a depth of 12 cm. This ion chamber produces a greater current flow for the electrometer to detect, per unit radiation exposure. Therefore, it exhibits greater sensitivity to low levels of bremsstrahlung. The depth of 12 cm simulates the middle of a 24 cm thick patient. The absolute dose is determined by the following equation:

$$\text{Dose} = \frac{R \cdot C}{M} \cdot C_{\lambda} \cdot \frac{760}{P} \cdot \frac{T + 273.15}{295.15} \cdot f$$

where R is the electrometer reading in Coulombs, C is the calibration factor, M is the number of accelerator monitor units used to achieve R, C_{λ} is the roentgen-to-rad conversion factor for photons, P is atmospheric pressure in mm Hg, T is temperature in C°, and f is the conversion from rads in water to rads in tissue. Substituting appropriate values into the equation, yields the following expression:

$$\text{Dose} = \frac{(0.0133 \times 10^{-8} C)\,(57.24 \times 10^{8}\ \text{rad/C}}{999\ \text{Monitor Units}} \cdot (0.94)(0.935)(1)(0.99)$$

Dose = 0.0005634 rad/MU or about 0.56 mRads/MU

In calculating the dose of the patient, the normal treatment regimen is utilized as a guide. The number of monitor units per position, the six treatment positions per two-day cycle, the meter reading (the sum of the individual +20°

and -20° values), and the number of irradiation cycles administered, are all factored into the final dose calculation as shown below:

Total Dose = (Σ R)(1200 M.U./Position)(6 positions/cycle)(17.5 cycles/3500 rad e^{-})

Thus,

Total Dose = (0.0005634)(1200)(6)(17.5) = 70.98 ≈ 71 rads

This indicates that the center of the hypothetical patient received a total x-ray dose through the course of treatment of 71 rads.

The dose to the patient at a height of 6'2" was measured by the same method to be more than twice as much dose, 148 rads for the treatment. At the patient's feet, about 3" above the platform base, the dose was measured to be 103 rads.

Therefore, it has been shown that the dose near the center of the vertical axis of the patient is much less than the dose at the patient's head or feet. Determining the exact shape of this curve to examine the change in dose with the distance from the mid-point is desirable and worthy of further research.

VITA

Alan G. Douglas was born 23 August, 1949, in Syracuse, New York. He attended Griffith Institute and Central School in Springville, New York, graduating in 1967.

In that same year he matriculated at North Carolina Wesleyan College. He graduated in 1971 with a B.S. in Biology and a concurrent B.A. in Chemistry.

Following graduation, he entered the U. S. Coast Guard and received a Commission. He currently holds the rank of Lieutenant Commander in the U.S. Coast Guard Reserve.

Upon release from active duty in 1975, he joined the Florida Department of Health, Radiological Health Section. In 1979, he moved to Baton Rouge to work with the Louisiana Nuclear Energy Division. While there he began to pursue part-time studies at L.S.U., his interest in Medical Physics having been sparked by various short courses offered to health physics personnel by the USNRC and various states and contractors.

In August of 1982, the author returned to the academic world as a full-time student to train as a clinical physicist.

He is presently a candidate for the degree of Master of Science offered through the Nuclear Science Center, Louisiana State University and Agricultural and Mechanical College.